

Journal Pre-proof



Taxifolin stability: In silico prediction and in vitro degradation with HPLC-UV/UPLC–ESI-MS monitoring

Fernanda Cristina Stenger Moura, Carmem Lúcia dos Santos Machado, Favero Reisdorfer Paula, Angélica Garcia Couto, Maurizio Ricci, Valdir Cechinel-Filho, Tiago J. Bonomini, Louis P. Sandjo, Tania Mari Bellé Bresolin

PII: S2095-1779(19)31011-1

DOI: <https://doi.org/10.1016/j.jpha.2020.06.008>

Reference: JPHA 568

To appear in: *Journal of Pharmaceutical Analysis*

Received Date: 19 November 2019

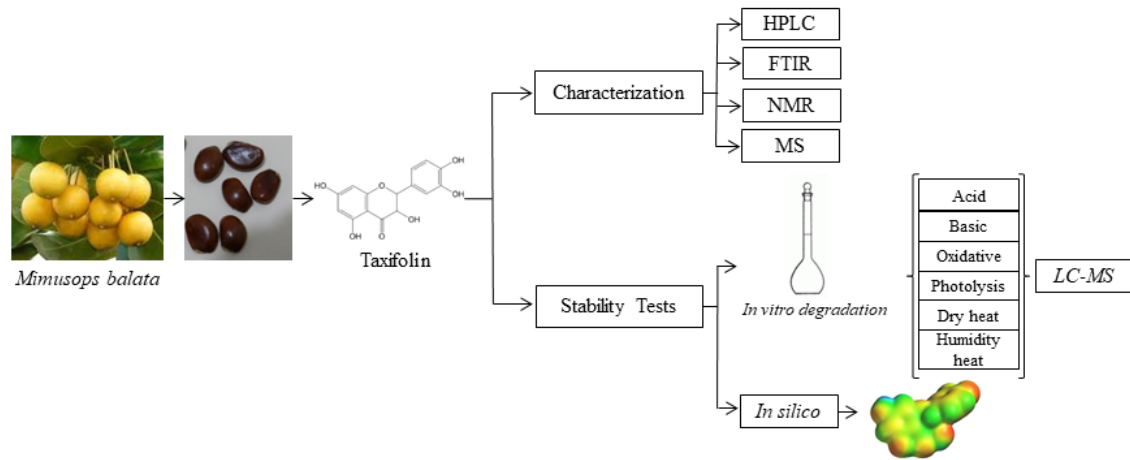
Revised Date: 28 June 2020

Accepted Date: 29 June 2020

Please cite this article as: F.C. Stenger Moura, C. Lúcia dos Santos Machado, F.R. Paula, Angé.Garcia. Couto, M. Ricci, V. Cechinel-Filho, T.J. Bonomini, L.P. Sandjo, T.M. Bellé Bresolin, Taxifolin stability: In silico prediction and in vitro degradation with HPLC-UV/UPLC–ESI-MS monitoring, *Journal of Pharmaceutical Analysis* (2020), doi: <https://doi.org/10.1016/j.jpha.2020.06.008>.

This is a PDF file of an article that has undergone enhancements after acceptance, such as the addition of a cover page and metadata, and formatting for readability, but it is not yet the definitive version of record. This version will undergo additional copyediting, typesetting and review before it is published in its final form, but we are providing this version to give early visibility of the article. Please note that, during the production process, errors may be discovered which could affect the content, and all legal disclaimers that apply to the journal pertain.

© 2020 Xi'an Jiaotong University. Production and hosting by Elsevier B.V. All rights reserved.



1 **Taxifolin stability: in silico prediction and in vitro degradation with HPLC-**
2 **UV/UPLC–ESI-MS monitoring**

3 Fernanda Cristina Stenger Moura¹, Carmem Lúcia dos Santos Machado², Favero
4 Reisdorfer Paula², Angélica Garcia Couto¹, Maurizio Ricci³, Valdir Cechinel-Filho¹,
5 Tiago J. Bonomini¹, Louis P. Sandjo⁴, Tania Mari Bellé Bresolin^{1*}.

6
7 ¹ *Pharmaceutical Sciences Graduate Program, Pharmacy Course, Universidade do*
8 *Vale do Itajaí - UNIVALI, Itajaí - SC, 88302-202, Brazil.*

9 ² *Laboratory of Research and Development of Drugs. Course of Pharmacy.*
10 *Pharmaceutical Sciences Graduate Program. Universidade Federal do Pampa -*
11 *UNIPAMPA, Uruguaiana - RS, 97500-970. Brazil.*

12 ³ *Department of Pharmaceutical Science – Università degli Studi di Perugia – UniPg,*
13 *via del Liceo 1, Perugia (PG), Italy.*

14 ⁴ *Department of Chemistry, Universidade Federal de Santa Catarina – UFSC,*
15 *Trindade, Florianópolis - SC, 88040-900, Brazil*

16
17 ***Corresponding author: T.M.B. Bresolin**

18 Fone/Fax: (+55) 47 3341-7930

19 Email adress: tbresolin@univali.br

20 ORCID: <https://orcid.org/0000-0002-4200-9201>

21
22 **ABSTRACT**

23 Taxifolin has a plethora of therapeutic activities and is currently isolated from the stem
24 bark of the tree *Larix gmelinni* (Dahurian larch). It is a flavonoid of high commercial
25 interest, for use in supplements or in antioxidant-rich functional foods. However, their
26 poor stability and low bioavailability hinder the use of flavonoids in nutritional or

27 pharmaceutical formulations. In this work, Taxifolin isolated from the seeds of
28 *Mimusops balata*, was evaluated by in silico stability prediction studies and in vitro
29 forced degradation tests (acid and alkaline hydrolysis, oxidation, visible/UV radiation,
30 dry/humid heating) monitored by HPLC-UV and UPLC-ESI-MS. The in silico stability
31 prediction tests indicated the most susceptible regions in the molecule to nucleophilic
32 and electrophilic attacks, as well as the sites susceptible to oxidation. The in vitro forced
33 degradation tests were in agreement with the in silico stability prediction, indicating that
34 Taxifolin is extremely unstable (class 1) under alkaline hydrolysis. In addition,
35 Taxifolin thermal degradation was increased by humidity. On the other hand, with
36 respect to photosensitivity, Taxifolin can be classified as class 4 (stable). Moreover, the
37 alkaline degradation products were characterized by UPLC-ESI-MS/MS as dimers of
38 Taxifolin. These results enabled an understanding of the intrinsic lability of Taxifolin,
39 contributing to the development of stability-indicating methods, and of appropriate drug
40 release systems, with the aim of preserving its stability and improving its
41 bioavailability.

42

43 **Keywords:** dihydroquercetin, in silico stability prediction; forced degradation.

44

45 1. Introduction

46 Taxifolin, also called dihydroquercetin, was first isolated from *Pseudotigusa*
47 *taxifolia* [1]. It belongs to the class of dihydroflavonoids, which are present as a yellow
48 pigment in many edible plants. Lavitol[®], an enriched extract of the stem bark of *Larix*
49 *gmellini*, contains about 90% Taxifolin. This natural product has been marketed and
50 used as a food ingredient in the USA since 2009 [2]. It has been recently authorized as a

51 novel food ingredient in Europe [3]. Taxifolin has been reported in more than 700
52 articles published in the literature.

53 Taxifolin (3,5,7,3',4'-pentahydroxyflavanone, or dihydroquercetin) is a potent
54 antioxidant, comparable to alpha-tocopherol, whose mechanism of action consists of
55 lipid radical scavenging [4]. Taxifolin presents several pharmacological properties, such
56 as attenuating diabetic nephropathy, reducing sugar, uric acid and creatinine in human
57 blood [5], decreasing the accumulation of β -amyloid and preventing memory deficits
58 [6], protecting against oxidative stress [7], promoting osteogenic differentiation in
59 human bone marrow mesenchymal stem cells [8], reducing blood viscosity and dilating
60 the blood vessels, and reducing arterial hypertension [9]. It also helps prevent diabetic
61 cardiomyopathy [10] and protects against alcoholic liver steatosis [11]. Its *in vivo*
62 gastroprotective effects were also demonstrated by our research group, with a similar
63 effect to omeprazol, inhibiting 41% of the pump effect [12]. Due to its relevant
64 pharmacological activities, this potential phytodrug was previously incorporated into
65 gastro adhesive microparticles for the treatment of gastric disorders, by our research
66 group [13].

67 However, despite its high clinical application potential, there is no sufficient data
68 on its stability, a key quality statement for a drug. On the other hand, there are few
69 stability studies carried out with natural products [14]. Previous studies revealed that
70 Taxifolin polymerizes when submitted to electrolysis in neutral solutions (pH 7.0) [15].
71 This substance is also considered to be highly slightly soluble in water, and its absolute
72 bioavailability after oral administration of lipid solution was only 36% [16]. Some
73 authors argue that the results for absorption profile and the parameters of Taxifolin vary
74 quite considerably, suggesting that the bioavailability of the compound depends on the
75 source [3]. This compound also appears to be degraded by the intestinal microflora [17].

76 Based on the above, the investigation of the Taxifolin stability behavior is an important
77 step in the development of a new active pharmaceutical ingredient (API), and for
78 stimulating the development of a potential new drug release system. Moreover, the
79 detection of potential degradation products requires stability-indicating methods [18]
80 and the application of forced degradation tests of the API candidate, in both solid and
81 solution forms. The stress condition should be carefully selected, aiming to generate
82 potential degradation products, which are likely to be formed under realistic storage
83 conditions [19].

84 Therefore, Taxifolin stability was investigated using *in silico* stability prediction
85 studies and *in vitro* forced degradation studies, monitoring the formation of degradation
86 products by HPLC-UV and UPLC-ESI-QTOF-MS.

87

88 **2. Experimental**

89

90 *2.1. Chemicals and reagents*

91 Methanol and acetonitrile of LC-UV and LC-MS grade were obtained from
92 PanReac, Castellar del Vallès, Barcelona Spain. Phosphoric acid of analytical grade was
93 purchased from Dinâmica, Sao Paulo, Brazil. Class 1 water was obtained by
94 ultrapurification (Direct-Q®, Merck KGaA, Darmstadt, Germany). All the solutions
95 were filtered through a regenerated cellulose 0.45 and 0.22 µm membrane filter
96 (Macherey-Nagel, Düren, Germany) prior to injection into HPLC and UPLC,
97 respectively. The Taxifolin used in this experiment was isolated from the seed of
98 *Mimusops balata* (from Itajaí, Santa Catarina, Brazil) with 99.4% purity (estimated by
99 HPLC), and characterized by ¹H and ¹³C NMR, infrared spectroscopy, HPLC and mass
100 spectrometry (Supplementary Material).

101

102 2.2. *In silico stability prediction studies*

103 Computational analyses were performed using Spartan 08 version 116.2® for Windows
104 (Wave function, Inc., USA) and all initial structures were constructed using fragments
105 of atoms and structural fragments by the molecular editor. Geometric optimization was
106 carried out using the Merck Molecular Strength Field (MMFF94) followed by the
107 Austin Model. The structure of Taxifolin (Fig. 1A-B) was subjected to conformational
108 analysis. The increment of the torsion angle was 30° in a range of 0-360°, using
109 systematic analysis, by the functional density theory (DFT) method to B3LYP/6,311G *
110 (d, f). The lowest energy conformer calculated was re-optimised using the same method.
111 This structure was used to determine the number of electrons at natural atomic
112 population analysis (NPA) using single point energy at the same level of theory of
113 geometry optimisation. For these data, FF derivatives values, positive (f_j , Eq. 1) for
114 electrophilic attack, negative (f_j^+ , Eq. 2) for nucleophilic attack and f^0_j (Eq. 3)-, for
115 radical attack are calculated as follows:

116
$$f^-_j = qj(N) - qj(N - 1) \quad (1)$$

117
$$f^+_j = qj(N + 1) - qj(N) \quad (2)$$

118
$$f^0_j = \frac{1}{2} qj [(N + 1) - qj(N - 1)] \quad (3)$$

119 The possible regions of the molecule susceptible to degradation, under acid and alkaline
120 conditions, were evaluated by the Fukui functions [20]. These functions indicate the
121 susceptibility of the electronic density to deform at a given position upon accepting or
122 donating electrons [21]. In this case, qj is the number of electrons (evaluated from NPA)
123 at the j th atomic site in the neutral (N), anionic ($N + 1$) or cationic ($N - 1$) chemical
124 species on the reference molecule.

125 The dual descriptor $\Delta f(\mathbf{r})$ of local reactivity, which allows us to obtain a
 126 preferred locus for nucleophilic attacks ($\Delta f(\mathbf{r}) > 0$) and a preferred electrophilic attack
 127 site ($\Delta f(\mathbf{r}) < 0$) in the system at point \mathbf{r} , was calculated using the equation 4 [22, 23].

$$128 \quad \Delta f(\mathbf{r}) = f^+(\mathbf{r}) - f^-(\mathbf{r}) \quad (4)$$

129 The main mechanism of auto-oxidation observed in the photolytic degradation
 130 reaction of the hydrogen atom abstraction energy was calculated for the bond of the
 131 hydrogen atom with the carbon atom, bond dissociation energy (BDE) in the molecule,
 132 using the equation 5 [24,25].

$$133 \quad (BDE)_{EH \text{ abstraction}} = E_{\text{radical}} + E_{H\text{radical}} - E_{\text{ground state}} \quad (5)$$

134

135 2.3. HPLC-UV methodology

136 The chromatographic profile, purity and extractive content were analyzed by HPLC
 137 (Prominence LC-20AT LC, Shimadzu, Tokyo, Japan) equipped with a binary pump, a
 138 photo diode array detector (SPD-M20A, Shimadzu), an auto-sampler (SIL-20AHT,
 139 Shimadzu) in-line degasser (DGU-20A5, Shimadzu), a column oven (CTO-10AS V,
 140 Shimadzu), a 20 μ L stainless steel loop and the software Class VP (version 6.14).

141 The analyses were carried out with a column Kinetex® F5 (Phenomenex, Torrance,
 142 California, USA; 150 mm x 4.6 mm, 2.6 μ m) conditioned at 30 °C, with detection at
 143 288 nm. The best gradient elution (0.6 mL/min) was acidified water pH 3.0 with
 144 phosphoric acid 0.1% (V/V) (A), acetonitrile (B) and methanol (C) according to the
 145 following gradient A:B:C (V/V): 85:10:5 to 80:15:5 (0-5 min); 80:15:5 to 70:25:5 (5-15
 146 min); 70:25:5 to 50:45:5 (15-25 min); 50:45:5 to 85:10:5 (25-30 min), maintaining these
 147 conditions until 35 min.

148 The HPLC-UV methodology was validated for linearity, limits of detection (LOD)
 149 and quantification (LOQ), robustness and selectivity. To access the linearity, Taxifolin

150 was dissolved in methanol in the range of 5.0-100.0 $\mu\text{g/mL}$, in triplicate, followed by
151 linear regression studies, using Excel software. The LOQ and LOD were determined
152 based on the standard deviation of the response and the slope [26]. Selectivity of the
153 method for Taxifolin was proven firstly by accessing the resolution (R) between the
154 Taxifolin peak and the nearest peak (impurity) in the original sample. Secondly, the
155 methodology was applied to quantify the Taxifolin among the degradation products
156 after the stress tests, measuring the purity peak of Taxifolin through the PDA detector.
157 To check the robustness of the method, the flow (± 0.06 mL/min), temperature (± 1 $^{\circ}\text{C}$)
158 and storage time of the sample solution were varied (3, 8, 12 and 24 h) measuring the
159 relative standard deviation (RSD) of the analyte content. The Taxifolin content was
160 calculated using the regression linear equation.

161

162 2.4. *Forced degradation studies*

163 Firstly, an aliquot of Taxifolin (1 mg) was dissolved in 1 mL of methanol. Then, the
164 volume was completed, to 5 mL, with the respective solvent of each forced degradation
165 test. Hydrolytic stress studies were performed in acid medium (1 M HCl) and the
166 mixture was maintained for 15, 30, 60, 240 min and 24 h. Taxifolin was also treated
167 with an alkaline condition, at 1 mM NaOH, during 15, 30, 60, 240 min and 24 h.
168 Oxidative tests were carried out in 30% H_2O_2 for 15, 30, 60, 240 min and 24 h. All the
169 stress experiments were carried out at 25 $^{\circ}\text{C}$. The final concentration of Taxifolin in the
170 respective degradation media was 200 $\mu\text{g/mL}$. Acid and alkaline samples were
171 neutralized with NaOH and HCl, respectively, and prior to HPLC analysis, the sample
172 solutions were diluted with methanol to 100 $\mu\text{g/mL}$. This concentration was chosen in
173 order to improve the appearance of the degradation products in the HPLC-UV
174 chromatograms. To LC-MS analysis, Taxifolin was submitted to 0.01 M NaOH

175 degradation at room temperature, followed by immediate neutralization with equimolar
176 HCl. The Taxifolin powder was stored in a photostability chamber (model 91423, ZEM,
177 Minas Gerais, Brazil) under combined visible light (1.2 and 2.4 million lux.h) and UVA
178 (200 and 400 Wh/m² irradiation). The negative control was protected with aluminium
179 foil coating. The light intensity was monitored by a Luximeter (model MLM-1011,
180 Minipa, São Paulo, Brazil). The samples were also stored in an oven at 40 °C and at
181 40°C/75% RH (into a desiccator with saturated solution of NaCl) for 30 days [27]. After
182 exposure to light, heat and humidity, sample solutions of 100 µg/mL in methanol were
183 analysed by HPLC. All stressed samples were assayed by comparison with non-
184 degraded reference standards in the same concentration, in methanol, to calculate the %
185 of degradation.

186

187 *2.5 UPLC-ESI-HRMS/MS analysis*

188

189 LC-MS analyses were performed on an Acquity UPLC system class H (Waters)
190 composed of a PDA detector, sample manager and a quaternary solvent manager as well
191 as an Acquity UPLC BEH C18 column (Waters; 130 Å, 1.0 mm x 50 mm, particle size
192 1.7 µm). Temperatures of 40 °C and 20 °C were set for the column and sample tray,
193 respectively. A volume of 3 µL was injected for each sample, and the separation was
194 obtained in a gradient condition [1-5 min 95% A (water/formic acid, 99.9/0.1 [V/V])
195 and 5% B (ACN), 5–8 min, 80% A, 8–10 min 50% A, 10–13 min 45% A, 13-16 min
196 10% A, 16-20 min 95% A] at a flow rate of 0.3 mL/min.

197 Mass detection was conducted on a Xevo G2-S QToF (Waters) with an electrospray
198 probe operating in negative ionization mode; nebulizer gas: nitrogen, cone gas flow 60
199 L/h; desolvation gas flow 900 L/h, sampling cone 40 V, source offset 80 V; collision

200 gas, argon. Lockspray reference sample was Leucine enkephalin with reference mass at
201 m/z 554.2615 (ESI-). Temperatures of 300 °C and 120 °C were used for the desolvation
202 and for the cone, respectively, while the capillary voltage was 3 kV. The collision
203 energy was 30 eV. Data were acquired in a range of 100-1500 Da, at a scan time of 1.0 s
204 during 20 min, and were processed with Mass Lynx V4.1 (Waters).

205

206 3. Results and discussion

207

208 The isolated and purified Taxifolin was characterized by FTIR spectra
209 (supplementary material, Fig. S1), mass spectrometry data (supplementary material,
210 Fig. S2) and ^1H NMR spectral data (supplementary material, Fig. S3) and then,
211 submitted to the stress tests.

212

213 3.1. LC-UV method validation

214 The method was linear in the range of 5.0-100.0 $\mu\text{g/mL}$ ($y = 113027x - 67233$, $r^2 =$
215 0.9989). The LOD and LOQ were 4.6 and 15.9 $\mu\text{g/mL}$, respectively. The
216 chromatographic conditions showed selectivity with high resolution ($R = 4.2$) between
217 the Taxifolin and the nearest peak (impurity identified as a Taxifolin isomer), showing a
218 high purity peak index of 0.999973, through the PDA detector. The method was robust
219 for changes in temperature (RSD of 0.25%), mobile phase flow (RSD of 0.47%), and
220 also for storage time (RSD of 0.47%), with $p > 0.05$, showing no statistical difference in
221 the Taxifolin assay in the small and deliberate modifications of the methodology,
222 compared to the standard condition.

223

224 3.2. *In silico stability prediction study*

225

226 Taxifolin stability was first investigated by in silico prediction studies and after by
227 in vitro forced degradation tests, monitoring the samples by HPLC-UV and UPLC-ESI-
228 HRMS/MS.

229 In silico stability prediction studies were performed to further understanding of the
230 chemical reactivity by predicting the most likely position of structural hydrolysis. The
231 chemical structure (Fig.1A) in the tube model (Fig. 1B) and the map of electrostatic
232 potential charges (MEP) (Fig. 1C) of Taxifolin are shown in Fig. 1. The MEP plot
233 calculated on the van der Waals surface and focusing on the negative isopotential
234 surfaces might be used to describe the occurrence of the electronic conjugation in the
235 molecule. The most negative potential regions are demonstrated in red to oxygen atoms.
236 The benzene ring shows no coplanarity with the chromen-4-ene ring, but the oxygen
237 atoms from chromen-4-ene and hydroxyl (O10) moieties and benzene attached to
238 position C2 showed a mesomeric effect. The center of the structure presents extended
239 distribution of negative charges, which become more positive as the potential increases
240 to hydrogen attached to oxygen atoms from hydroxyl moieties.

241

Fig.1

242 As shown in Table 1, the major values of the Fukui function ($f_{(r)}$) are those with
243 higher reactivity [28], whose sites may be related to hydrolysis reactions during stress
244 degradation studies. Table 1 also showed that positions C2, C4, and C7 were more
245 susceptible to undergo nucleophilic attack. According to the dual descriptor $\Delta f(\mathbf{r})$
246 results, the following order was observed: C4>C7>O10>C8, indicating preferably the
247 chromen-4-one ring and C2' (Fig. 1) in benzene ring sites as the most reactive ($\Delta f(\mathbf{r})>0$)

248 into the system at point **r**. All molecular regions, especially C4 and C7, were shown to
249 be the most probable reactive sites to alkaline or acid hydrolysis (Table 1, Fig. 1).

250 **Table 1**

251 The Fukui function f^0 and BDE, used to estimate the hydrogen abstraction energies,
252 indicate the auto-oxidation of Taxifolin shown in Table 2. Fukui function showed a high
253 value for the hydrogen atom of C2' in the chemical structure of Taxifolin (Fig. 1),
254 indicating the main region of susceptibility in the oxidation process. However, this
255 hydrogen atom is stabilized by the resonance effect, and may not easily receive an
256 electron in auto-oxidation, which suggests that the mechanism of electron transfer is not
257 related to Taxifolin chemical structure oxidation.

258 **Table 2**

259 BDE is a measure of the bond strength in a chemical bond, and may be defined as
260 the standard energy (or even the enthalpy) change when a bond is broken by a reaction
261 [29]. BDE is an indicator of primary site(s) of the auto-oxidation of organic compounds
262 and drugs [25]. Low BDE values of hydrogen atoms from the Taxifolin structure (Table
263 2) are more liable to be abstracted from the auto-oxidation reaction. The energies of
264 hydrogen atoms attached to C2 and C3 from the chromen-4-ene ring and O7' and O8'
265 from hydroxyl moieties attached to the para-position of the benzene ring (Fig. 1) reflect
266 the high oxidative susceptibility that characterizes the instability of this region in the
267 oxidative environment. On the other hand, the hydrogen atom from C8 showed a high
268 BDE calculated value, indicating that this molecular position moiety is more stable in
269 the studied conditions. The mesomeric effect observed in this structural region may can
270 hinder the abstraction of this hydrogen. This procedure can be used for auto-oxidation
271 and also for predicting photolytic degradation [30].

272 The Fukui function was previously used to estimating the antioxidant mechanism of
273 Taxifolin, compared to quercetin [31]. However, the authors studied only the hydrogen
274 atoms attached to oxygen atoms, and showed that in oxidant medium, Taxifolin
275 exhibited more susceptibility to hydrogen loss at O3' and O4', which corresponds to the
276 O7' and O8' position denominated in the present work (Fig. 1A). Thus, these findings
277 are in agreement with the results demonstrated here, considering the hydroxyl moieties.

278 On the other hand, forced degradation studies are recommended as part of stability
279 studies for new drugs because the molecule is exposed to extreme conditions during its
280 manufacturing, storage, and administration. Thus, to simulate the appearance of
281 potential degradation products, stress tests are useful and allow us to establish the
282 degradation pathways and the intrinsic stability of the molecule, and to validate a
283 stability-indicating method. The Guideline ICH Q1A(R2) [27] states that the molecule
284 should be exposed to high temperatures, humidity, oxidation, photolysis, and
285 susceptibility to hydrolysis across a range of pH values, in solution or suspension.

286

287 3.3. Forced degradation tests

288

289 Taxifolin was submitted to forced degradation studies, selecting the condition which
290 provides about 10 – 20% of degradation [27].

291 The Taxifolin degradations, for each stress condition, were: 20.2% (1 M HCl, 30
292 min), 16.3% (1 mM NaOH, 15 min), 11.7% [30% (V/V) H₂O₂, 24 h], 9.8% (dry heat, at
293 40°C, 30 days), 23.1% (Humid heat, at 40 °C and 75% RH, 30 days) and 9.0%
294 (photolysis at 2.4 million lux.h and at 400 Wh/m² of visible and UVA radiation,
295 respectively). Taxifolin was shown to be extremely unstable (class 1) [32] under
296 alkaline hydrolysis. Taxifolin degradation was increased by humidity, compared with

297 dry heat, probably due to the hydrolysis process in the former condition. The stability of
298 a semi-solid formulation containing Taxifolin was also evaluated [33]. After 12 weeks,
299 at 40 °C, only 3% of the initial amount was found, which is in agreement with the
300 results of the present study, reinforcing the thermolability of this compound, especially
301 in the presence of humidity. Under oxidative conditions, Taxifolin could be classified as
302 class 4 (stable), with a relative low photosensitivity [32]. Thus, according to the above
303 results, Taxifolin needs to be protected against these stress conditions with a proper
304 formulation, avoiding intestinal delivery in particular.

305 The chromatographic profile of Taxifolin showed changes after being subjected to
306 certain degradation conditions, with the appearance of supplementary peaks (Fig. 2).
307 The Taxifolin used for the stress studies showed low levels of impurity (0.6%) (Fig.
308 2A). In this original sample, four impurity peaks eluted after the major Taxifolin peak
309 (Fig. 2A1). The acidic hydrolysis tests with 1 M HCl showed supplementary peaks with
310 earlier elution, decreasing from the major peak, as well as the disappearance of impurity
311 peaks, which probably suffered acid hydrolysis (Fig. 2B). Alkaline tests were performed
312 starting at 1M NaOH, followed by 0.1 M NaOH and in both conditions, Taxifolin was
313 completely decomposed, as evidenced by the UV profile of the peak with a retention
314 time of 18 min. Decreasing the concentration to 0.01 M NaOH, 75% Taxifolin
315 degradation was observed, and as the contact time increased, this degradation was
316 completed (supplementary material, Fig. S4).

317 Thus, the chosen conditions to LC-UV analysis, for alkaline degradation, were 1
318 mM NaOH for 15 min (Fig. 2C). Oxidation with 30% (V/V) H₂O₂ resulted in a decrease
319 in Taxifolin and a change of chromatographic profile, with many earlier eluted peaks
320 (Fig. 2D). Samples were also submitted to dry heat (40 °C) (Fig. 2E) and humid heat (40
321 °C/75% RH) for 30 days (Fig. 2F), without important chromatographic profile changes.

322 Finally, Taxifolin was submitted to combined daylight fluorescent lamp and ultraviolet
323 (UVA) (Fig. 2G), showing photostability.

324 **Fig.2**

325

326 UPLC-ESI-HRMS-MS analysis was used to characterize the degradation products
327 of Taxifolin present in samples obtained from various conditions of degradation
328 including alkaline medium (Fig. 3).

329 **Fig.3**

330 The samples were more sensitive to negative ionization mode using the base peak
331 ion (BPA) as the mode of acquisition of the chromatograms [34]. The first
332 chromatogram obtained from the Taxifolin sample (Fig. 3A) displayed seven peaks,
333 with the most intense one at 6.47 min, with a shoulder at 6.62 min, both with the base
334 peak ion m/z 303.0515 corresponding to $[C_{15}H_{12}O_7-H]^-$ calculated for m/z 303.0505 (Δ
335 3.37 ppm). The second peak at 6.62 min exhibited the same molecular ion, suggesting a
336 Taxifolin diastereomer. This suggestion was supported by fragment ions observed in the
337 MS/MS spectra of both compounds at m/z 285.04 $[C_{15}H_{12}O_7-H_2O]^-$ and 125.02
338 (corresponding to phloroglucinol: ring A). The peak at 7.54 min with the pseudo-
339 molecular ion m/z 301.0367 $[C_{15}H_{10}O_7-H]^-$ (Δ 6.22 ppm) was assigned as quercetin
340 based on the fragment ion observed at m/z 151.01 formed by the Retro-Diels-Alder
341 rearrangement of ring C. This molecule is an oxidized form of Taxifolin. The other
342 peaks at 8.79, 10.73, 11.17, and 14.77 min did not give fragment ions that would enable
343 their characterization. However, the last metabolite at 14.77 min (m/z 281.2484
344 $[C_{18}H_{34}O_2-H]^-$ Δ 1.23 ppm) was assigned as oleic acid derivative.

345 In addition to the metabolites already present in the Taxifolin sample, acid
346 hydrolysis produced two new metabolites. The first was observed at 0.46 min

347 (molecular ion m/z 197.79) and the second at 7.10 min (molecular ion m/z 723.51). The
348 latter peak also appeared in the alkaline, oxidative and dry thermal degradation of
349 Taxifolin (Table 3). Diagnostic analysis of the MS/MS data of this peak was not
350 conclusive.

351 Sample oxidative test showed in its LCMS data features similar to those of acid
352 degradation, with the exception of an additional peak at 0.49 min with m/z 162.88. The
353 humidity thermal test afforded a sample for which LCMS analysis gave two peaks, at
354 12.46 min and 13.34 min, with m/z 325.18 and m/z 339.19, respectively. The structure
355 of m/z 325.18 could not be assigned, whereas based on a literature search m/z 339.1976
356 $[\text{C}_{22}\text{H}_{28}\text{O}_3\text{-H}]^-$ (Δ 4.66 ppm) is related to a steroid. These metabolites are probably
357 contaminants of the starting material, and appear during the degradation process, which
358 decreased the concentration of the main compounds

359 The sample from dry thermal degradation afforded in its LCMS data peaks at 12.57
360 and 14.47 min with the same mass value m/z 439.24; Because of the lack of fragment
361 ions on the MS/MS spectrum, the structure of this metabolite could not be assigned.
362 However, a literature search revealed that m/z 439.24 is related to a steroid.

363 In the UV photolysis sample, a peak was observed at 8.28 min with m/z 221.1180
364 $[\text{C}_{13}\text{H}_{18}\text{O}_3\text{-H}]^-$ (Δ 1.04 ppm), like in visible photolysis. A search using this elemental
365 composition led to a structure related to norsesquiterpene. An additional peak was also
366 observed at 12.60 min (m/z 421.2301) with no relation to Taxifolin. Some peaks that
367 appear in the water conditions are probably degradation products of quercetin, because
368 in acid, alkaline, oxidative, and dry thermic degradation, the peak at 7.54 min, for which
369 the molecular ion is m/z 301.03, disappeared. In addition, these samples, when analyzed
370 by HPLC, did not show a significant decrease in the Taxifolin peak (Fig. 2).

371

Table 3

372 The purest Taxifolin sample (99%) was submitted to alkaline hydrolysis,
373 specifically at 0.01 M NaOH for LCMS analysis, and neutralized to afford, in its LC-
374 MS analysis, a peak at 7.25 min flanked with m/z 603.0787 [$C_{30}H_{20}O_{14}-H$]⁻ (calc. m/z
375 603.0775, Δ 2.02 ppm) (Fig. 3B), suggesting the dimerization of Taxifolin. The same
376 chromatogram also showed the presence of a substance at 4.86 min with m/z 319.0456
377 [$C_{15}H_{12}O_8-H$]⁻ (Calc. m/z 319.0454, Δ 0.65 ppm), differing from the Taxifolin chemical
378 composition (m/z 303 [$C_{15}H_{12}O_7-H$]⁻) by 16 Da. This substance may be a product
379 formed from the oxidation of Taxifolin by oxygen (1O_2) (Fig. 4).

380 Fig.4

381 As ring B is more susceptible to oxidation than ring A [35], it was suggested that
382 alkaline degradation involves the auto-oxidation promoted by the radical peroxide
383 formation. After losing a molecule of water and forming a ketone group, the aromatic
384 system of B ring was rebuilt, resulting in the ion m/z 319.0456 (Fig. 4A). UPLC-ESI-
385 MS² data of this product showed fragment ions at m/z 193, 195, 153 and 163 (Fig. S5,
386 supplementary material) supported this hypothesis and indicated that oxidation occurred
387 on B ring of the flavanone.

388 The second peak with m/z 337.0568 [$C_{15}H_{14}O_9-H$]⁻ (calc. m/z 337.0560, Δ 2.50
389 ppm), observed at 6.18 min (Fig. 3B), differed from m/z 319.0456 by 18 Da,
390 corresponding to an H₂O molecule (Fig. 4A). It was suggested that this compound was a
391 result of the oxidation of ring B of Taxifolin and the opening of ring C. The tandem
392 mass spectra of this second product showed a base peak ion of m/z 125 and a radical
393 anion m/z 152. The fragmentation proposal in Fig. S5 (supplementary material) revealed
394 that m/z 125 could be related to A and B rings, whereas m/z 163 was produced by the
395 sigma bond cleavage at the α -carbon atom. This latter fragmentation also indicated that
396 ring C was opened.

397 The third and fourth peaks, with m/z 605.0964 [$C_{30}H_{22}O_{14}-H$]⁻ (calc. m/z 605.0931,
398 Δ 5.40 ppm), at 6.99 and 7.43, min, respectively, were indicative of dimeric products of
399 Taxifolin. It was suggested that these dimers were formed by 2 moles of Taxifolin in the
400 alkaline medium, which reacted with one mol of O₂ to produce 2 moles of Taxifolin
401 anion radical and H₂O₂. Furthermore, radical delocalization led to the formation of two
402 dimeric flavanones (Fig. 4B). Similar oxidative dimerization was electrochemically
403 produced by Chernikov et al. [15]. The tandem mass spectrum of both compounds (m/z
404 605.0964) showed similar fragments at m/z 393, m/z 259 and m/z 217. The ion m/z 393
405 was obtained by the elimination of one chromenone moiety and H₂O. While the loss of
406 two chromenone units produced m/z 217, the product ion m/z 259 was obtained from the
407 opening of C ring and the loss of a chromenone unit (Fig. S6, supplementary material).

408 The product at m/z 603.0787 differs from m/z 605.0964 by 2 uma, suggesting
409 oxidation by O₂ (Fig. 4C). In addition, the oxidation could produce an *ortho*-quinone
410 dimeric flavanone, thus like a quercetin molecule, which has a similar structure to
411 Taxifolin, differing only in the double bond between C2 and C3. Quercetin also
412 showed susceptibility to pH, temperature and storage conditions, generating the same
413 *ortho*-quinone, which can interact with glutathione and may explain its high antioxidant
414 effect [36]. The latter, when analyzed by tandem mass spectrometry, generated ions at
415 m/z 409, 391, 381, 193, and 177, demonstrating that oxidation occurred on the B ring
416 and not on the C ring (Fig. S6, supplementary material).

417

418 4. Conclusions

419 Thus, *in silico* stability prediction analysis suggested that the Taxifolin molecule
420 is susceptible to nucleophilic attack in C2', C4 and C7, as confirmed by the *in vitro*
421 alkaline degradation, suggesting that the molecular ion with m/z 603.0787 and m/z

422 605.0964 could be Taxifolin dimers via nucleophilic attack in C2' for both molecules.
423 The degradation products formed are also susceptible to nucleophilic attack. Other
424 carbons are also previewed to be susceptible to nucleophilic attack, with less
425 probability, but in vitro forced degradation studies proved that secondary degradation
426 could occur. In the m/z 319 peak fragmentation, the nucleophilic attack occurred in C4
427 and O12 (m/z 167), in C2, C3, and O12 (m/z 153), in C2 and O12 (m/z 193) and in C2
428 and O12 (m/z 195), which corroborates the in silico stability prediction for susceptibility
429 in C2, C4 and O12. In the m/z 337 fragmentations, the nucleophilic attack occurred in
430 C2', C4 (m/z 125) and in C2, O12 and C4 (m/z 125), in O1, O12 (m/z 163), in C2 and
431 C3 (m/z 152), in agreement with in silico stability prediction for C2', C2, C4, O12.
432 Thus, the in silico stability prediction study should be predictive to the reactivity
433 susceptibility of Taxifolin in the studied conditions, contributing to the understanding of
434 Taxifolin intrinsic lability and guiding the development of appropriate release systems
435 for this phytodrug.

436 **Acknowledgments:** This work was partially supported by CAPES (PVE, grant
437 88887.116106/2016- 00) (Coordenação de Aperfeiçoamento de Pessoal de Nível
438 Superior), Brazil, which provided financial support in the form of a doctoral's degree
439 scholarship to Stenger, F. C. and financial support (Science Program Without Borders -
440 Researcher Special Visitor – PVE), and CNPq (Conselho Nacional de Desenvolvimento
441 Científico e Tecnológico), Edital Universal (grant 88887.122964/2016- 00).

442

443 **Conflicts of interest:** The authors declare that there are no conflicts of interest

444

445 **References**

- 446 [1] H.M. Graham, E.F. Kurth, Constituents of extractives from douglas fir, Ind. Eng.
447 Chem. 41 (1949) 409-414. <https://doi.org/10.1021/ie50470a035>.
- 448 [2] A.G. Schauss, S.S. Tselyico, V.A. Kuznetsova, et al., Toxicological and
449 genotoxicity assessment of a dihydroquercetin-rich dahurian larch tree (*Larix*
450 *gmelinii* Rupr) extract (Lavitol), Int. J. Toxicol. 34 (2015) 162-181.
451 <https://doi.org/10.1177/1091581815576975>.
- 452 [3] F. Schlickmann, L.M. Mota, T. Boeing, et al., Gastroprotective bio-guiding of fruits
453 from *Mimusops balata*, Naunyn Schmiedebergs Arch. Pharmacol. 388 (2015)
454 1187-1200. <https://doi.org/10.1007/s00210-015-1156-8>.
- 455 [4] D. Turck, J-L. Bresson, B. Burlingame, et al., Scientific opinion on taxifolin-rich
456 extract from Dahurian Larch (*Larix gmelinii*), EFSA J. 15 (2017) 1-16.
457 <https://doi.org/10.2903/j.efsa.2017.4682>.
- 458 [5] J.O. Teselkin, B.A. Zhambalova, I.V. Babenkova, et al., Antioxidant properties of
459 dihydroquercetin, Biofizika. 41 (1996) 620–624.
- 460 [6] Y. Zhao, W. Huang, J. Wang, et al., Taxifolin attenuates diabetic nephropathy in
461 streptozotocin-induced diabetic rats, Am. J. Transl. Res. 10, (2018), 1205-1210.
462 PMID: [PMCID: PMC5934579](https://pubmed.ncbi.nlm.nih.gov/305934579/)
- 463 [7] Y. Wang, Q. Wang, X. Bao, et al., Taxifolin prevents β -amyloid-induced
464 impairments of synaptic formation and deficits of memory via the inhibition of
465 cytosolic phospholipase A₂/prostaglandin E₂ content, Metab. Brain. Dis. 33 (2018)
466 1069-1079. <https://doi.org/10.1007/s11011-018-0207-5>.
- 467 [8] X. Xiaobin, J. Feng, Z. Kang, S. et al., Taxifolin protects RPE cells against oxidative
468 stress-induced apoptosis, Mol. Vis. 23 (2017)520-528. PMID: [PMCID: PMC5534490](https://pubmed.ncbi.nlm.nih.gov/305534490/)
- 469 [9]. Y.J. Wang, H.Q. Zhang, H.L. Han, et al., Taxifolin enhances osteogenic
470 differentiation of human bone marrow mesenchymal stem cells partially via NF κ B

- 471 pathway, *Biochem. Biophys. Res. Commun.* 490 (2017) 36-43.
472 <https://doi.org/10.1016/j.bbrc.2017.06.002>.
- 473 [10] M.B. Plotnikov, O.I. Aliev, A.V. Sidekmenova, et al., Modes of hypertension
474 action of dihydroquercetin in arterial hypertension, *Bul. Exp. Biol. Med.* 162
475 (2017) 353-356. <https://doi.org/10.1007/s10517-017-3614-4>.
- 476 [11]. X. Sun, R. Chen, Z. Yang, et al., Taxifolin prevents diabetic cardiomyopathy in
477 vivo and in vitro by inhibition of oxidative stress and cell apoptosis, *Food Chem.*
478 *Toxicol.* 63 (2014) 221-232. <https://doi.org/10.1016/j.fct.2013.11.013>.
- 479 [12] Y. Zhang, Q. Jin, X. Li, et al., Modulation of AMPK-dependent lipogenesis
480 mediated by P2x7R-NLRP3 inflammasome activation contributes to the
481 amelioration of alcoholic liver steatosis by dihydroquercetin, *J. Agric. Food Chem.*
482 16 (2018) 4862-4871. <https://doi.org/10.1021/acs.jafc.8b00944>
- 483 [13] F.C. Stenger Moura, L. Perioli, C. Pagano, et al., Chitosan composite
484 microparticles: A promising gastroadhesive system for taxifolin, *Carbohydr. Pol.*
485 218 (2019) 343-354. <https://doi.org/10.1016/j.carbpol.2019.04.075>
- 486 [14] J.H.S. Gomes; G.C. da Silva; S.F. Côrtes; et al., Forced degradation of L -(+)-
487 bornesitol, a bioactive marker of *Hancornia speciosa*: Development and validation
488 of stability indicating UHPLC-MS method and effect of degraded products on ACE
489 inhibition, *J. Chromatogr. B* 1093 (2018) 31-
490 38. <https://doi.org/10.1016/j.jchromb.2018.06.045>
- 491 [15] D.A Chernikov, T.A. Shishlyannikova, A.V. Kashevskii, et al., Some peculiarities
492 of taxifolin electrooxidation in the aqueous media: The dimers formation as a key
493 to the mechanism understanding, *Electrochim. Acta* 271 (2018) 560-566.
494 <https://doi.org/10.1016/j.electra.2018.02.179>.

- 495 [16] O.N. Pozharitskaya, M.V. Karlinab, A.N. Shikov, et al., Determination and
496 pharmacokinetic study of taxifolin in rabbit plasma by high-performance liquid
497 chromatography, *Phytomedicine* 16 (2009) 244–251.
498 <https://doi.org/10.1016/j.phymed.2008.10.002>.
- 499 [17] J. Winter, L.H. Moore, V.R. Dowell, et al., C-ring cleavage of flavonoids by
500 human intestinal bacteria, *Appl. Environ. Microbiol.* 55 (1989) 1203–1208.
501 PMID:[2757380](https://pubmed.ncbi.nlm.nih.gov/2757380/)
- 502 [18] M. Blessy, R.D. Patel, P.N. Prajapati, et al., Development of forced degradation
503 and stability indicating studies of drugs—A review, *J. Pharm. Anal.* 4 (2014) 159-
504 165.<https://doi.org/10.1016/j.jpha.2013.09.003>.
- 505 [19] M.M. Annapurna, C. Mohapatro, A. Narendra, Stability-indicating liquid
506 chromatographic method for the determination of Letrozole in pharmaceutical
507 formulation, *J. Pharm. Anal.* 2 (4) (2012) 298–
508 305.<https://doi.org/10.1016/j.jpha.2012.01.010>.
- 509 [20] J. Kieffer, E. Brémond, P. Lienard, et al., In silico assessment of drug substances
510 chemical stability, *J. Mol. Struct.* 954 (2010)75–
511 79.<https://doi.org/10.1016/j.theochem.2010.03.032>.
- 512 [21] L.H. Mendoza-Huizar, Global and local reactivity descriptors for picloram
513 herbicide: a theoretical quantum study, *Quim. Nova* 38 (2015) 71-76.
514 <https://doi.org/10.5935/0100-4042.20140283>.
- 515 [22] C. Cárdenas, N. Rabi, P. Ayers, et al., Chemical reactivity descriptors for
516 ambiphilic reagents: dual descriptor, local hyper softness, and electrostatic
517 potential, *J. Phys. Chem. A.* 113 (2009) 8660-8667. [https://doi.org/
518 10.1021/jp902792n](https://doi.org/10.1021/jp902792n).

- 519 [23] C. Morell, A. Hocquet, A. Grand, et al., A conceptual DFT study of hydrazino
520 peptides: Assessment of the nucleophilicity of the nitrogen atoms by means of the
521 dual descriptor $\Delta f(r)$, J. Mol. Struct. Theochem. 849 (2008) 46-51.
522 <https://doi.org/10.1016/j.theochem.2007.10.014>.
- 523 [24] T.R. Sharp, Calculated carbon-hydrogen bond dissociation enthalpies for
524 predicting oxidative susceptibility of drug substance molecules, Int. J. Pharm. 418
525 (2011) 304-307. <https://doi.org/10.1016/j.theochem.2005.01.028>.
- 526 [25] P. Lienard, J. Gavartin, G. Boccardi, et al., Predicting drugs substances
527 autoxidation, Pharm. Res. 32 (2015) 300-310. [https://doi.org/10.1007/s11095-014-](https://doi.org/10.1007/s11095-014-1463-7)
528 [1463-7](https://doi.org/10.1007/s11095-014-1463-7).
- 529 [26] ICH, Harmonized Tripartite Guideline Specifications: Validation of analytical
530 procedures: text and methodology Q2(R1), Current Step 5 version, 2005.
- 531 [27] ICH, Harmonised Tripartite Guideline Stability Testing: Photostability Testing of
532 New Drug Substances and Products Q1B, Current Step 4 version, 1996.
- 533 [28] R.G. Parr, W. Yang, Functional Theory of Atoms and Molecules, Oxford Univ.
534 Press, New York, 1989.
- 535 [29] S.J. Blanksby, G.B. Ellison, Bond dissociation energies of organic molecules, Acc.
536 Chem. Res. 36 (2003) 255-263. <https://doi.org/10.1021/ar020230d>.
- 537 [30] S. Yamada, Y. Naito, M. Takada, et al., Photodegradation of hexachlorobenzene
538 and theoretical prediction of its degradation pathways using quantum chemical
539 calculation, Chemosphere 70 (2008) 731-736. <https://doi.org/>
- 540 [31] E. Osorio, E. G. Pérez, C. Areche, et al., Why is quercetin a better antioxidant than
541 taxifolin? Theoretical study of mechanisms involving activated forms, J. Mol. Model.
542 19 (2013) 2165-2172.

- 543 [32] S. Singh, M. Bakshi, Guidance on conduct of stress test to determine inherent
544 stability of drugs, *Pharm. Technol.* 24 (2000) 1-14.
- 545 [33] H.J. An, Y. Lee, L. Liu, et al., Physical and Chemical Stability of Formulations
546 Loaded with Taxifolin Tetra-octanoate, *Chem. Pharm. Bull.*, 67, 1 (2019), 985-991.
- 547 [34] S. Barrek, O. Paisse, M.F. Grenier-Loustalot, Analysis of neem oils by LC-MS and
548 degradation kinetics of azadirachtin-A in a controlled environment, *Anal. Bioanal.*
549 *Chem.*, 3 (2004) 753-763.
- 550 [35] M. Mocek, P.J. Richardson, Kinetics and mechanism of quercetin oxidation, *J. Inst.*
551 *Brew.* 78 (1972) 459-465. <https://doi.org/10.1002/j.2050-0416.1972.tb03481.x>.
- 552 [36] W. Wang, C. Sun, L. Mao, et al. The biological activities chemical stability,
553 metabolism and delivery system of quercetin: A review, *Trend Food Sci.* 56 (2016)
554 21-38. <https://doi.org/10.1016/j.tifs.2016.07.004>.

555

556 **Figure Captions**

557

558 **Fig. 1.** Chemical structure of Taxifolin (A); 3D visualization in tube (B); Molecular
559 Electronic Potential (MEP) (C), beyond the van der Waals isosurface 0.002 eV using
560 Spartan for Windows 08. Color scheme: blue positive to red negative electrostatic
561 potentials values (-40.000 e75.000 kcal/mole).

562 **Fig. 2.** Chromatograms of Pristine Taxifolin (A and A1) and of Taxifolin degraded with
563 1 M HCl, 30 min (B), 1 mM NaOH, 15 min (C), 30% H₂O₂, 24 h (D), dry heat, 30 days
564 (E), humid heat, 30 days (F) and photolysis, 2.4 million lux.h (G).

565 **Fig. 3.** LC-MS of Pristine Taxifolin (A) and the alkaline forced degradation (0.01 M
566 NaOH immediately neutralized with equimolar HCl) of Tax (B).

567 **Fig. 4.** Hypothetical alkaline degradation mechanism of Taxifolin with 0.01 M NaOH
568 leading to m/z 319.0456 and m/z 337.0568 (A); m/z 605.0964 (B); m/z 603.0787 (C).

569

570 **Table captions**

571

572 **Table 1.** Values of the NPA (neutral, positive and negative populational analysis),
573 Electrophilic f^- and nucleophilic f^+ condensed Fukui functions and $\Delta f(\mathbf{r})$ of the atoms of
574 the Taxifolin molecule calculated with the DFT/B3LYP and the 6,311G* (d, f) basis set
575 considering equations 1, 2, and 3.

576 **Table 2.** Fukui function values for radical attack and bond dissociation energies of
577 Taxifolin hydrogen

578 **Table 3.** Degradation products of Taxifolin after exposition to different stress
579 conditions, monitored by UPLC-ESI-MS.

580

Table 1.

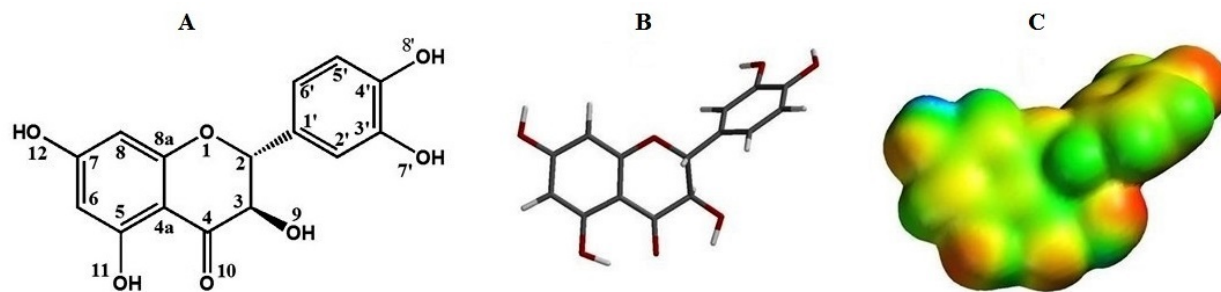
Atoms	NPA	NPA ⁺	NPA ⁻	f^+	f	$\Delta f(\mathbf{r})$
O1	8.52946	8.49859	8.55921	-0.03087	-0.02975	-0.00112
C2	5.92398	5.93919	5.92735	0.015207	-0.00337	0.01858
C3	5.97847	5.97604	5.96088	-0.00243	0.01759	-0.02002
C4	5.47298	5.47368	5.67386	0.000698	-0.20088	0.20158
C4a	6.32195	6.32146	6.29739	-0.00048	0.02456	-0.02505
C5	5.57605	5.56164	5.64018	-0.01440	-0.06414	0.04973
C6	6.37703	6.28324	6.39284	-0.09378	-0.01582	-0.07797
C7	5.61044	5.61768	5.71376	0.007233	-0.10332	0.11055
C8	5.59928	5.58731	5.68196	-0.01198	-0.08268	0.07071
C8a	6.40131	6.34162	6.40806	-0.05968	-0.00675	-0.05294
O9	8.75674	8.75092	8.78593	-0.00582	-0.02919	0.02337
O10	8.62877	8.59317	8.75514	-0.03559	-0.12637	0.09077
O11	8.68331	8.62974	8.73394	-0.05357	-0.05064	-0.00293
O12	8.67417	8.65064	8.71821	-0.02353	-0.04404	0.02051
C1'	6.08394	5.99073	6.05584	-0.09321	0.02801	-0.12130
C2'	6.29342	6.29690	6.30145	0.00348	-0.00804	0.01152
C3'	5.73766	5.67456	5.74815	-0.06309	-0.01050	-0.05259
C4'	5.70828	5.64012	5.73460	-0.06816	-0.02632	-0.04184
C5'	6.27564	6.25328	6.29178	-0.02236	-0.01614	-0.00623
C6'	6.22217	6.17170	6.22733	-0.05047	-0.00516	-0.04531
O7'	8.72534	8.66951	8.73926	-0.05583	-0.01391	-0.04192
O8'	8.69390	8.60099	8.71253	-0.09291	-0.01863	-0.07428

Table 2.

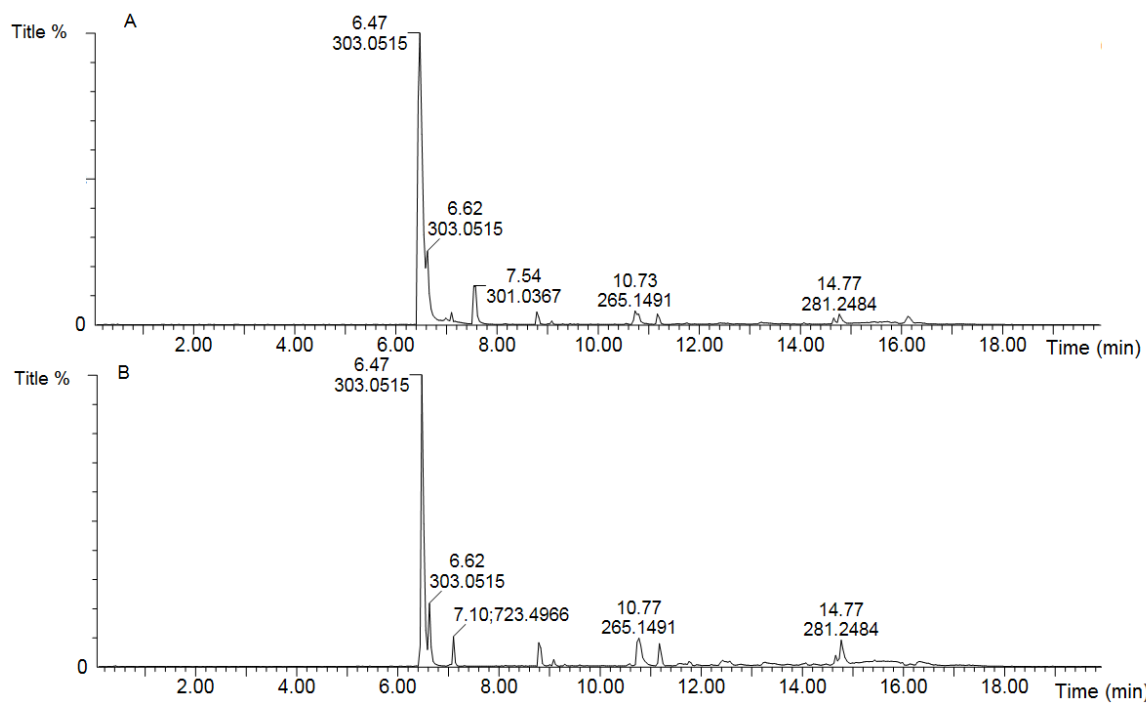
Hydrogen atoms	f^0	<i>BDE</i> (EH abstraction) Kcal mole ⁻¹
H-C2	-0.02141	70.4797
H-C3	-0.02848	73.1857
H-C6	-0.03022	110.8045
H-C8	-0.02669	123.2532
H-C2'	-0.01148	105.5393
H-C5'	-0.02537	105.8795
H-C6'	-0.01725	103.9090
H-O9	-0.01293	102.8659
H-O11	-0.00893	107.5006
H-O12	-0.01873	107.5006
H-O7'	-0.01459	74.5874
H-O8'	-0.01546	77.9537

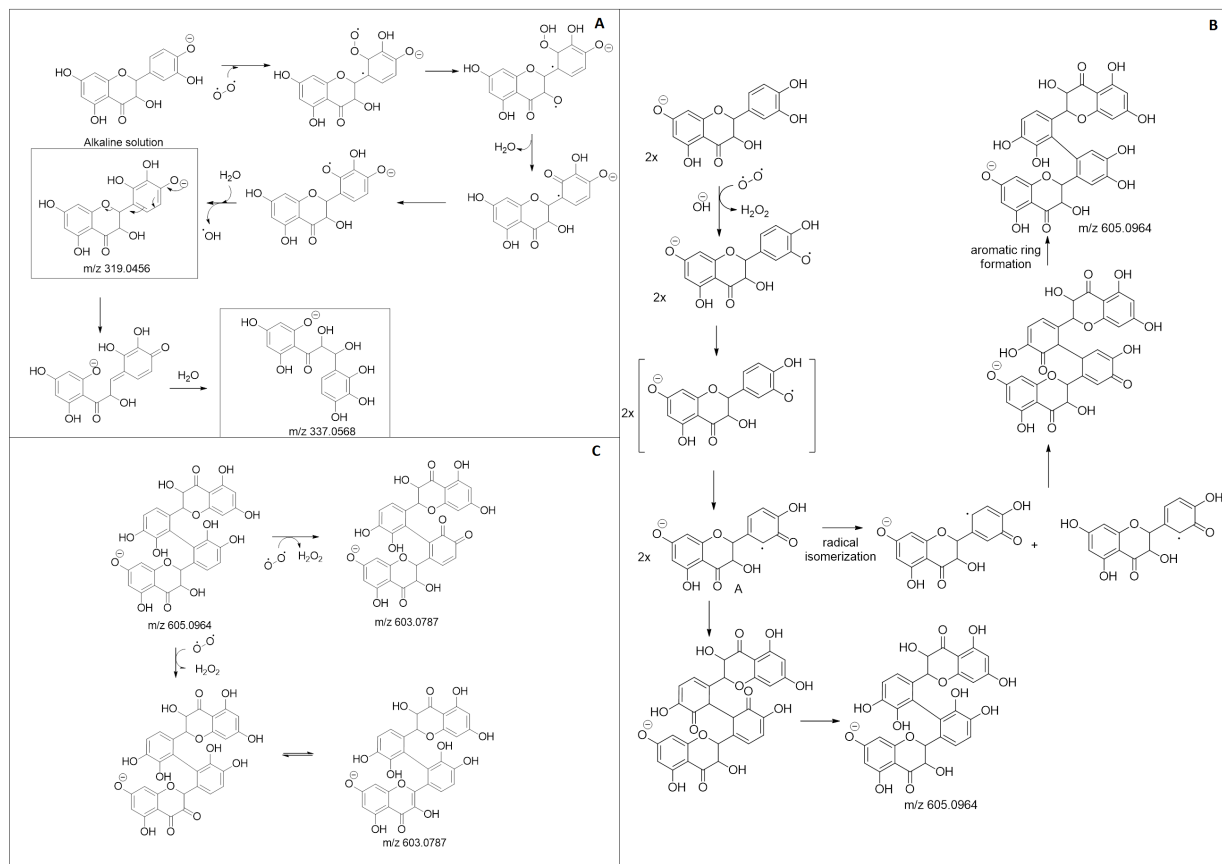
Table 3.

Peak No.	RT (min)	Negative ion mode (<i>m/z</i>) MS [M- H] ⁻									Elem. Comp.
		Taxifolin	Stress condition								
			NaOH 1mM	HCl 1M	H ₂ O ₂ 30%	Visible light (2.4 mi lux h ⁻¹)	Vis. neg control	Light	Humid heat 40°C, 75% RH	Dry heat 40°C	
1	0.46	-	-	197.79	-	-	-	-	-	-	C ₇ H ₃ O ₇
2	0.49	-	-	-	162.89	-	-	-	-	-	C ₆ H ₁₀ O ₅
3	6.47	303.05	303.05	303.05	303.06	303.05	303.05	303.06	303.05	303.05	C ₁₅ H ₁₂ O ₇
4	6.62	303.05	303.05	-	-	303.05	303.05	-	-	-	C ₁₅ H ₁₂ O ₇
5	7.10	-	723.50	723.501	723.51	-	-	723.52	-	-	CHO
6	7.54	301.04	-	-	-	301.04	301.04	-	301.03	-	C ₁₅ H ₁₀ O ₇
7	8.42	-	-	-	-	-	-	-	265.14	-	CHO
8	8.82	-	-	-	-	221.12	221.12	-	-	-	CHO
9	10.77	265.15	265.15	265.15	265.151	265.15	265.15	265.15	265.15	265.15	CHO
10	12.46	-	-	-	-	-	-	-	325.18	-	
11	12.57	-	-	-	-	-	-	439.25	-	-	CHO
12	12.60	-	-	-	-	421.23	-	-	-	-	CHO
13	13.34	-	-	-	-	-	-	-	339.20	-	CHO
14	14.47	-	-	-	-	-	-	439.25	-	-	
15	14.77	281.25	281.25	281.24	281.25	281.25	281.25	-	281.25	-	CHO



Journal Pre-proof





Journal Pre-proof

Highlights

- An stability-indicating HPLC-UV method was developed to Taxifolin.
- Taxifolin showed high *in silico* susceptibility to nucleophilic attack.
- Taxifolin is unstable under acid, oxidative and especially alkaline conditions.
- Alkaline degradation products were characterized by UPLC-ESIMS/MS.

Journal Pre-proof